Ⓔ

ON MEASURING THE INFRARED LUMINOSITY OF DISTANT GALAXIES WITH THE *SPACE INFRARED TELESCOPE FACILITY*

CASEY PAPOVICH AND ERIC F. BELL[1]
Steward Observatory, University of Arizona, 933 North Cherry Avenue, Tucson AZ 85721;
papovich@as.arizona.edu, ebell@as.arizona.edu

ABSTRACT

The *Space Infrared Telescope Facility* (*SIRTF*) will revolutionize the study of dust-obscured star formation in distant galaxies. Although deep images from the Multiband Imaging Photometer for *SIRTF* (MIPS) will provide coverage at 24, 70, and 160 μm, the bulk of MIPS-detected objects may only have accurate photometry in the shorter wavelength bands because of the confusion noise. Therefore, we have explored the potential for constraining the total infrared (IR) fluxes of distant galaxies solely with the 24 μm flux density and for the combination of 24 and 70 μm data. We also discuss the inherent systematic uncertainties in making these transitions. Under the assumption that distant star-forming galaxies have IR spectral energy distributions (SEDs) that are represented somewhere in the local universe, the 24 μm data (plus optical and X-ray data to allow the redshift estimation and AGN rejection) constrain the total IR luminosity to within a factor of 2.5 for galaxies with $0.4 \lesssim z \lesssim 1.6$. Incorporating the 70 μm data substantially improves this constraint by a factor $\lesssim 6$. Lastly, we argue that if the shape of the IR SED is known (or well constrained, e.g., because of a high IR luminosity or a low ultraviolet/ IR flux ratio), then the IR luminosity can be estimated with more certainty.

Subject headings: cosmology: observations — galaxies: high-redshift — infrared: galaxies

On-line material: color figures

1. INTRODUCTION

The evolution of the global, volume-averaged star formation rate (SFR) is currently a topic of intense interest (see, e.g., Madau et al. 1996; Steidel et al. 1999; Yan et al. 1999; Haarsma et al. 2000). Observationally, a galaxy's SFR must be inferred from the luminosity density at wavelengths dominated by young stars, such as the ultraviolet (UV), nebular emission lines, mid- to far-infrared (IR), or radio (see, e.g., Kennicutt 1998; Condon 1992), and by making assumptions about the form of the initial mass function. Because of dust, rest-frame UV/optical indicators often underestimate the intrinsic SFR, especially for more luminous galaxies (see, e.g., Calzetti, Kinney, & Storchi-Bergmann 1994; Calzetti 2001; Bell 2002). Based on the UV/optical spectral energy distributions (SEDs) and far-IR emission of distant galaxies and QSOs, dust appears to be prevalent in high-redshift objects ($z \sim 2$–5; e.g., Pettini et al. 1998; Adelberger & Steidel 2000; Carilli et al. 2000; Papovich, Dickinson, & Ferguson 2001; Chapman et al. 2002). Dust reprocesses the energy absorbed from the UV/optical into the mid/far-IR, and thus galaxy IR luminosities allow one to "balance the energy budget" and paint a much more complete picture of star formation throughout cosmic history (see, e.g., Sanders & Mirabel 1996; Blain et al. 1999; Flores et al. 1999).

The *Space Infrared Telescope Facility* (*SIRTF*), to be launched in 2003, offers to revolutionize our view at IR wavelengths with unprecedented sensitivity and resolution. Several cosmological surveys are being planned to obtain 24, 70, and 160 μm data with the Multiband Imaging Photometer for *SIRTF* (MIPS) (see, e.g., Lonsdale 2001; Dickinson & Giavalisco 2002; Rieke et al. 2001a, 2001b). The combination of these three bands will span the peak of the IR SEDs and will provide a fairly robust tracer of the total IR emission (e.g., Dale & Helou 2002). However, MIPS observations will rapidly become confusion-limited be-

cause of the increasing source density at faint fluxes (e.g., Xu et al. 2001; Dole, Lagache, & Puget 2002), especially for the longer wavelength data, which have lower sensitivity and resolution (MIPS resolution is roughly proportional to the bandpass central wavelength). Thus, full coverage of galaxies' IR SEDs with accurate photometry may only be possible for relatively nearby or bright objects.

In this Letter, we consider the uncertainties inherent in translating MIPS photometry into total IR fluxes in the case in which object photometry is only available from the shorter wavelength bands. The relation between mid-IR and far-IR is complex. Thus, we explore the connection between the 24 μm data and the total IR emission from both the observational (§ 2) and modeling (§ 3) perspective, with the assumption that local galaxy SEDs are representative of high-redshift analogs (which has not been robustly demonstrated, although see Adelberger & Steidel 2000 and Elbaz et al. 2002). In § 4, we investigate improving these constraints using 70 μm data, the galaxy luminosity, and/or UV flux. We summarize our results in § 5. Because extensive X-ray/ optical/near-IR coverage will be available for the majority of deep MIPS survey regions (see references above), we assume here that galaxies with dominant AGN contributions can be rejected using the X-ray data and that galaxies' redshifts (spectroscopic or photometric) will be known.

2. OBSERVATIONAL CONSTRAINTS BETWEEN THE MID-IR AND TOTAL IR EMISSION: THE CASE AT $z \sim 1$

To explore the correlation between mid-IR fluxes and the total IR flux[2] for local galaxies, we have taken data from the *Infrared Astronomical Satellite* (*IRAS*) at 12 μm. Note that the

---

[1] Present address: Max-Planck-Institut für Astronomie, Königstuhl 17, D-69117 Heidelberg, Germany; bell@mpia.de.

[2] We define the total IR flux as the integrated emission from 8 to 1000 μm, i.e., $F_{IR} \equiv F(8$–1000μm$)$, estimated using direct integration from 8 to 100 μm and extrapolated to 1000 μm using a λ^{-1} emissivity. These fluxes are typically a factor of 2 larger than those of Helou et al. (1988) and 30% higher than those of Sanders & Mirabel (1996), and they are consistent to within 10% with values extrapolated using 8–170 μm data from *IRAS* and Tuffs et al. (2002).

FIG. 1.—Ratio of the *IRAS* 12 μm to total IR flux (from 8 to 1000 μm) as a function the *IRAS* 100 μm–to–60 μm flux density ratio; see Bell (2002) for details. The symbols denote various galaxy types: starbursting galaxies (*open stars*), ultraluminous IR galaxies (*filled stars*), and normal galaxies (*open circles*). The error bar indicates typical uncertainties. Results for model galaxies are shown as lines (with line definitions as in Fig. 2).

FIG. 2.—Ratio of the observed MIPS 24 μm emission to total (rest frame) IR emission as a function of redshift. The curves display the models described in the text (labeled in upper left-hand corner). The arrow depicts galaxy SEDs from "warmer" to "colder" dust temperatures. [*See the electronic edition of the Journal for a color version of this figure.*]

MIPS 24 μm band in the observed frame for $z = 1$ nearly matches the rest-frame *IRAS* 12 μm band, with a *K*-correction that varies weakly with galaxy SED: $L_\nu(\text{MIPS } 24\ \mu\text{m}, z = 1) \approx 1.3 L_\nu(\text{IRAS } 12\ \mu\text{m}, z = 0)$.

Figure 1 shows the *IRAS* 12 μm–to–total IR flux ratio as a function of *IRAS* 100 μm–to–60 μm color for 156 galaxies spanning all star-forming types (Bell 2002).[3] The figure illustrates that a nearly constant proportion of the total IR flux emerges in the mid-IR for local galaxies. The mean ratio is $F(12\ \mu\text{m})/F_{\text{IR}} = 0.16$, with a 1 σ scatter between 0.10 and 0.22. This is consistent with *IRAS* and *Infrared Space Observatory* (*ISO*) results, which show a relatively constant conversion between rest-frame mid-IR (7–15 μm) and total IR luminosities (e.g., Spingolio et al. 1995; Chary & Elbaz 2001; Roussel et al. 2001). Clearly, in local galaxies, the dust responsible for the unidentified IR bands (UIBs; most plausibly associated with polycyclic aromatic hydrocarbons [PAHs]; e.g., Puget & Léger 1989; Genzel & Cesarsky 2000) that dominate the flux in the mid-IR correlates fairly well with the dust that produces the bulk of the total IR flux emission.

Importantly, Figure 1 shows that the ratio of 12 μm to total IR flux does not sensitively depend on the temperature of the dust that dominates at far-IR wavelengths [as measured by $f_\nu(100\ \mu\text{m})/f_\nu(60\ \mu\text{m})$]: the systematic variation with dust temperature seems to be smaller than the scatter. Overlaid in the figure are the results of models from the literature with different treatments of the mid/far-IR SEDs and that span a range of dust temperatures and IR luminosities (described in § 3). These models broadly reproduce the mean and scatter observed in the plot. These *IRAS* data suggest that if the relationship between the mid-IR and total IR emission at high redshifts is similar to
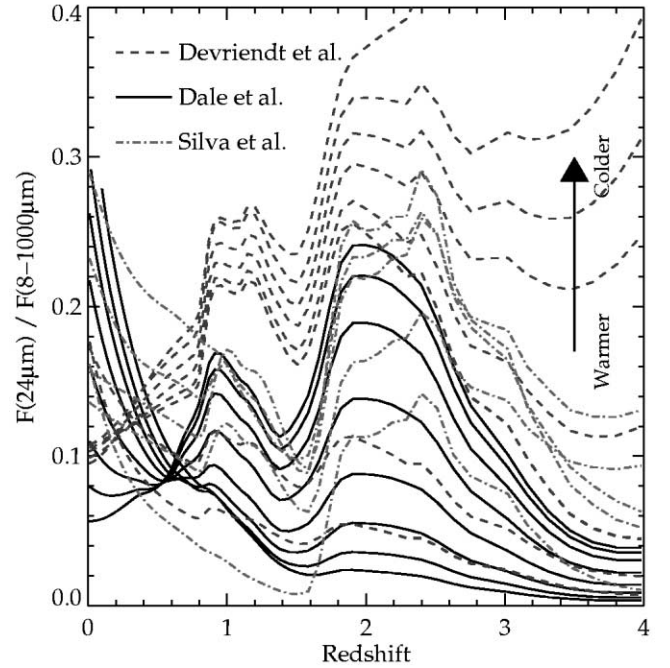
that observed locally, then the MIPS 24 μm data will provide an estimate to the total IR emission for $z \sim 1$ galaxies. Clearly, the scatter is significant (a factor of ≈2.5) and is largely systematic in the sense that it can only be improved on by better constraining the shape of the galaxy IR SED.

3. MODELING THE MID-IR TO TOTAL IR EMISSION: EXTENDING THE REDSHIFT RANGE

Here we turn to models to test the result from § 2 for a wider range of redshifts. In order to gauge the systematic model uncertainties, we explore three independently constructed sets of models: (1) We use the STARDUST templates for 17 local galaxies with a range of IR luminosities ($5 \times 10^9 \lesssim L_{\text{IR}}/L_\odot \lesssim 4 \times 10^{12}$ from Devriendt, Guiderdoni, & Sadat 1999). Note that the luminosities of the seven Virgo Cluster galaxies in this model were underestimated by a factor of between 10 and 300 (J. Devriendt 2002, private communication); this does not affect our results since we use only colors (flux ratios). (2) We have also used the fits of the GRASIL model of Silva et al. (1998) to six galaxies (Arp 220, M51, M82, M100, NGC 6090, and NGC 6946). (3) Lastly, we use the empirical models based on local galaxy *ISO* data from Dale et al. (2001) with a range of far-IR flux ratios (a surrogate for dust temperature), $-0.4 \lesssim \log F(60\ \mu\text{m})/F(100\ \mu\text{m}) \lesssim 0.5$. These models apply explicitly to local galaxy SEDs, and thus the caveat persists that they may not describe high-*z* galaxies.

To derive the observed-frame mid-IR flux as a function of redshift, we averaged the model galaxy SEDs with the MIPS 24 μm bandpass (including effects from the filter transmission and detector response) over a range of redshifts. In Figure 2, we show the ratio of the observed-frame MIPS 24 μm to rest-frame total IR flux versus redshift. As expected from the initial analysis of 12 μm *IRAS* data, the MIPS 24 μm emission is a fair tracer of the total (rest frame) IR emission, especially for

---

[3] We denote the average flux density measured from a bandpass with central wavelength λ as $f_\nu(\lambda)$, and we define the flux from the bandpass as $F(\lambda) \equiv \nu f_\nu(\lambda)$, where ν is the frequency corresponding to the wavelength λ.

the redshift range $0.4 \lesssim z \lesssim 1.6$, for which the scatter is a factor of 2–3.

It is worth discussing this in somewhat more detail. At $z \sim 0$, the observed 24 μm band traces emission from UIBs and from very small grains that have been transiently raised to high temperatures by absorption of single UV photons (Désert, Boulanger, & Puget 1990). Model SEDs show great variation in the prominence of this component, depending largely on the relative intensity of the UV radiation field in a given galaxy. As one moves toward $z \sim 1$–2.5, the MIPS 24 μm data probes lower rest-frame wavelengths where the UIBs increasingly contribute to the flux, especially in discrete features from ~ 7 to 13 μm (Genzel & Cesarsky 2000 and references therein). Empirically, these UIBs are rather more prominent for "cooler" galaxies with less intense UV radiation fields (causing the tracks for warmer and cooler galaxies to cross at $z \sim 0.5$). The "dip" in the 24 μm–to–total IR ratio at $z \sim 1.4$ is attributed to gaps between the UIBs. Silva et al. (1998), Devriendt et al. (1999), and Dale et al. (2001) model the UIBs somewhat differently. The largest difference between the models at $z \gtrsim 1$ is the contribution of the stellar continuum to the mid-IR emission. The galaxy templates match well for warm galaxies and diverge for cooler galaxies since Dale et al. (2001) do not have a large stellar contribution in their cold galaxies, whereas Devriendt et al. (1999) include seven Virgo Cluster galaxy templates that are dominated by stellar emission at $\lambda \lesssim 15$ μm (Boselli et al. 1998), and Silva et al. (1998) study three quiescently star-forming spiral galaxies (M100, M51, and NGC 6946) that contain some stellar contribution to the mid-IR emission. Certainly, the contribution of the old stellar population to dust heating is correlated with dust temperature (see, e.g., Bell 2002 and references therein); however, the scatter is large, leaving the issue of stellar contamination of $\lambda \lesssim 15$ μm fluxes largely open. Moreover, how these processes contribute to the IR SEDs of high-z galaxies is almost entirely unknown.

Given this (and with the inherent assumption that distant star-forming galaxies have IR SEDs that are represented somewhere in the local universe), one expects that at $0.4 \lesssim z \lesssim 1.6$, it should be possible to constrain the total IR flux to within a factor of 2–3 using 24 μm data alone: $F(24 \ \mu m)$ represents 5%–25% of the total IR flux. Outside this redshift range, the conversion is rather less certain. A factor of ≈ 2–3 in error in total IR flux may be quite adequate but can potentially frustrate many scientific analyses. Because this uncertainty is largely systematic, one must include additional knowledge of the shape of the galaxy SED in order to improve the constraint on the total IR flux.

4. IMPROVING THE TOTAL IR EMISSION CONSTRAINTS

Based on the models illustrated in Figure 2, the scatter between the 24 μm flux and the total IR flux emission stems primarily from a lack of knowledge of the shape of the galaxy IR SED (and/or dust temperature). MIPS 70 μm flux measurements will be available for a significant fraction of MIPS 24 μm sources (although the exact fraction and redshift distribution are strongly model-dependent), which should enhance the constraints on the total IR emission. Here we explore the constraints on the total galaxy IR emission in the case in which only MIPS 24 and 70 μm data are available. In Figure 3, we show the ratio of the observed MIPS 24 μm to total IR emission versus the ratio of the observed MIPS 24 μm to 70 μm fluxes in different redshift intervals. There is generally very little scatter in the relationship for these redshifts and colors: the ratio of the 24 μm to 70 μm fluxes seems to correlate with
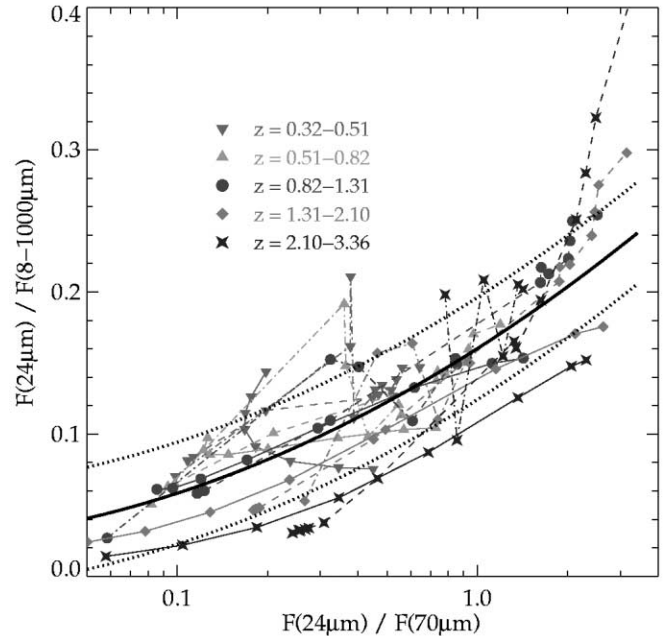
Fig. 3.—Ratio of the observed *SIRTF*/MIPS 24 μm emission to the total (rest frame) IR emission as a function of the MIPS 24 μm–to–70 μm flux ratio. The curves with symbols illustrate the various predictions from the models described in the text averaged over the redshift interval (as listed), with line styles as indicated in Fig. 2. The thick solid and dotted lines show a second-order polynomial fit and its standard error to the average over all model predictions and redshifts (see text). [*See the electronic edition of the Journal for a color version of this figure.*]

dust temperature over a wide range of redshifts. To crudely parameterize the relationship between the IR fluxes in these bandpasses, we have fitted a second-order polynomial to the average over all models for all redshifts shown in Figure 3. We find a best fit to the equation $F(24 \ \mu m)/F(8$–$1000 \ \mu m) = A + Bx + Cx^2$, where $x \equiv \log F(24 \ \mu m)/F(70 \ \mu m)$, with polynomial coefficients $A = 0.160$, $B = 0.135$, and $C = 0.033$ and a standard error of $\delta[F(24 \ \mu m)/F(8$–$1000 \ \mu m)] = 0.036$. This fit and error are overlaid in Figure 3. Our parameterization provides a means for quantifying the scatter in estimating the total IR flux emission using the MIPS 24 and 70 μm data (although the physical relation between these fluxes and the total IR emission is of course more complicated than this simple formalism), and it spans the systematic uncertainties inherent in the model predictions and is largely independent of redshift in the range $0.3 \lesssim z \lesssim 3.3$. Therefore, with both MIPS 24 and 70 μm detections (and with the assumption that local galaxy IR SEDs apply to high-redshift analogs), this result suggests that the uncertainty of the total IR flux is improved by up to a factor of ~ 6 (relative to that achieved using 24 μm data only).

Lastly, if distant luminous IR galaxies (LIRGs; $L_{IR} > 10^{11} \ L_{\odot}$) have comparable SEDs to those found locally, then it should be possible to better constrain the IR luminosity for this class of galaxy. Locally, LIRGs have "warmer" dust temperatures (Sanders & Mirabel 1996), thus allowing for a more robust conversion between observed 24 um and total IR luminosity (adopting the warmer tracks, with less stellar contribution, in Fig. 2). It may be possible to classify these galaxies as LIRGs on the basis of their high IR luminosities (indeed, although model-dependent, it may be the case that only LIRGs will be detectable in confusion-limited surveys for $z \gtrsim 1$; e.g., Dole et al. 2002). Alternatively, many local LIRGs have low UV-to-IR ratios, $F(1550 \ \text{Å})/F_{IR} < 0.02$,

which can be derived from observed-frame U-band–to–24 μm ratios for $z \sim 1$ galaxies, albeit in a model-dependent way. These conversions obviously depend sensitively on high-redshift LIRGs acting in similar ways to local LIRGs, which of course must be tested using spectral observations along with 70 and 160 μm photometry for the brightest galaxies.

5. CONCLUSIONS

SIRTF will greatly improve our understanding of the IR emission of (and hence the star formation processes within) distant galaxies. Because deep surveys could uncover many star-forming galaxies in the shorter wavelength MIPS data with no longer wavelength counterparts, we have explored the efficacy of constraining the total IR galaxy emission using the data at 24 μm only and the combination of 24 and 70 μm data (and under the assumption that ancillary optical and X-ray data are available to allow the redshift estimation and AGN rejection). Assuming that distant star-forming galaxies have IR SEDs that are represented somewhere in the local universe, the 24 μm data should constrain the integrated IR flux to within a factor of 2.5: $F(24 \ \mu\text{m})/F_{\text{IR}} \simeq 5\%$–$25\%$ for galaxies with $0.4 \lesssim z \lesssim 1.6$. Including MIPS 70 μm data, the IR luminosity can be estimated with considerably more certainty (a factor of $\lesssim 6$ improvement over the uncertainties using 24 μm data only). Lastly, if one can assume that the shape of the galaxy SED is similar to local luminous IR galaxies ($L \gtrsim 10^{11} \ L_{\odot}$; e.g., because of a high IR luminosity or a low UV/IR flux ratio), then the constraints should improve.

Throughout this study, we have made the explicit assumption that the relationships between the mid- and total IR emission and the shape of the IR SEDs observed locally apply to properties of high-redshift galaxies. As a final caveat, we emphasize that for many reasons, this may not be the case. Indeed, the population of IR-emitting galaxies must undergo strong evolution in order to match the cosmic IR background (Hauser & Dwek 2001; Chary & Elbaz 2001; Xu et al. 2001; Elbaz et al. 2002; Dole et al. 2002), and it is unclear how such evolution manifests itself. The mid-IR UIBs (e.g., PAHs) and total IR emission relation at high redshift may be different because of, e.g., a changing dust composition or because of a significantly different dust heating from older stellar populations than that observed locally. Moreover, we have assumed that the shape of the IR SED as a function of IR luminosity for local galaxies applies to high-redshift analogs, which is poorly known (although not inconsistent with observations; see, e.g., Adelberger & Steidel 2000). Only with large samples of galaxies detected in all three MIPS bands, and with spectroscopic measurements from the *SIRTF* Infrared Spectrograph, will these assumptions be testable. Once such constraints are established, the data should provide a prescription for relating the MIPS data to total IR fluxes. Given an estimate on the total IR luminosity, it is then possible to estimate the SFR (modulo the usual sources of uncertainty; see, e.g., Kennicutt 1998 and Bell 2002).

REFERENCES

Adelberger, K. L., & Steidel, C. C. 2000, ApJ, 544, 218
Bell, E. F. 2002, ApJ, submitted
Blain, A. W., Smail, I., Ivison, R. J., & Kneib, J.-P. 1999, MNRAS, 302, 632
Boselli, A., et al. 1998, A&A, 335, 53
Calzetti, D. 2001, PASP, 113, 1449
Calzetti, D., Kinney, A. L., & Storchi-Bergmann, T. 1994, ApJ, 429, 582
Carilli, C. L., et al. 2000, ApJ, 533, L13
Chapman, S. C., Shapley, A., Steidel, C., & Windhorst, R. 2002, ApJ, 572, L1
Chary, R., & Elbaz, D. 2001, ApJ, 556, 562
Condon, J. 1992, ARA&A, 30, 575
Dale, D. A., & Helou, G. 2002, ApJ, 576, 159
Dale, D. A., Helou, G., Contursi, A., Silbermann, N. A., & Kolhatkar, S. 2001, ApJ, 549, 215
Désert, F.-X., Boulanger, F., & Puget, J.-L. 1990, A&A, 237, 215
Devriendt, J. E. G., Guiderdoni, B., & Sadat, R. 1999, A&A, 350, 381
Dickinson, M., & Giavalisco, M. 2002, in ESO/USM Workshop, The Mass of Galaxies at Low and High Redshift, ed. R. Bender & A. Renzini (Berlin: Springer), in press (astro-ph/0204213)
Dole, H., Lagache, G., & Puget, J.-L. 2002, ApJ, submitted
Elbaz, D., Cesarsky, C. J., Chanial, P., Aussel, H., Franceschini, A., Fadda, D., & Chary, R. R. 2002, A&A, 384, 848
Flores, H., et al. 1999, ApJ, 517, 148
Genzel, R., & Cesarsky, C. J. 2000, ARA&A, 38, 761
Haarsma, D. B., Partridge, R. B., Windhorst, R. A., & Richards, E. A. 2000, ApJ, 544, 641

Hauser, M. G., & Dwek, E. 2001, ARA&A, 39, 249
Helou, G., Khan, I. R., Malek, L., & Boehmer, L. 1988, ApJS, 68, 151
Kennicutt, R. C., Jr. 1998, ARA&A, 36, 189
Lonsdale, C. J. 2001, BAAS, 198, 25.02
Madau, P., Ferguson, H. C., Dickinson, M., Giavalisco, M., Steidel, C. C., & Fruchter, A. S. 1996, MNRAS, 283, 1388
Papovich, C., Dickinson, M., & Ferguson, H. C. 2001, ApJ, 559, 620
Pettini, M., Kellogg, M., Steidel, C. C., Dickinson, M., Adelberger, K. L., & Giavalisco, M. 1998, ApJ, 508, 539
Puget, J.-L. & Léger, A. 1989, ARA&A, 27, 161
Rieke, G. H., et al. 2001a, BAAS, 199, 44.01
Rieke, M., et al. 2001b, in Deep Fields, ed. S. Cristiani, A. Renzini, & R. E. Williams (Berlin: Springer), 117
Roussel, H., Sauvage, M., Vigroux, L., & Bosma, A. 2001, A&A, 372, 427
Sanders, D. B., & Mirabel, I. F. 1996, ARA&A, 34, 749
Silva, L., Granato, G. L., Bressan, A., & Danese, L. 1998, ApJ, 509, 103
Spingolio, L., Malkan, M. A., Rush, B., Carrasco, L., & Recillas-Cruz, E. 1995, ApJ, 453, 616
Steidel, C. C., Adelberger, K. L., Giavalisco, M., Dickinson, M., & Pettini, M. 1999, ApJ, 519, 1
Tuffs, R. J., et al. 2002, ApJS, 139, 37
Xu, C., Lonsdale, C. J., Shupe, D. J., O'Linger, J., & Masci, F. 2001, ApJ, 562, 179
Yan, L., McCarthy, P. J., Freudling, W., Teplitz, H. I., Malumuth, E. M., Weymann, R. J., & Malkan, M. A. 1999, ApJ, 519, L47